

# Deep-Cavity Cavitand Octa Acid as a Hydrogen Donor: Photofunctionalization with Nitrenes Generated from Azidoadamantanes

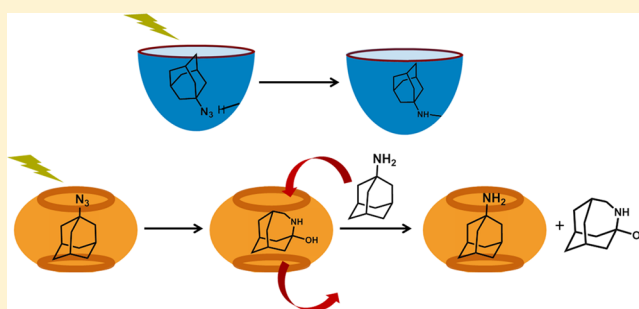
Rajib Choudhury,<sup>†</sup> Shipra Gupta,<sup>†</sup> José P. Da Silva,<sup>\*,‡</sup> and V. Ramamurthy<sup>\*,†</sup>

<sup>†</sup>Department of Chemistry, University of Miami, Coral Gables, Florida 33124, United States

<sup>‡</sup>Centro de Investigação em Química do Algarve, FCT, Universidade do Algarve, Campus de Gambelas, 8005-139 Faro, Portugal

## Supporting Information

**ABSTRACT:** 1-azidoadamantane and 2-azidoadamantane form a 1:1 complex with hosts octa acid (OA) and cucurbit[7]uril (CB7) in water. Isothermal titration calorimetric measurements suggest these complexes to be very stable in aqueous solution. The complexes have been characterized by <sup>1</sup>H NMR in solution and by ESI-MS in gas phase. In both phases, the complexes are stable. Irradiation of these complexes ( $\lambda > 280$  nm) results in nitrenes via the loss of nitrogen from the guest azidoadamantanes. The behavior of nitrenes within OA differs from that in solution. Nitrenes included within octa acid attack one of the four tertiary benzylic hydrogens present at the lower interior part of OA. While in solution intramolecular insertion is preferred, within OA intermolecular C–H insertion seems to be the choice. When azidoadamantanes included in CB7 were irradiated ( $\lambda > 280$  nm) the same products as in solution resulted but the host held them tightly. Displacement of the product required the use of a higher binding guest. In this case, no intermolecular C–H insertion occurred. Difference in reactivity between OA and CB7 is the result of the location of hydrogens; in OA they are in the interior of the cavity where the nitrene is generated, and in CB7 they are at the exterior. Reactivity of nitrenes within OA is different from that of carbenes that do not react with the host.



## INTRODUCTION

The value of deep-cavity cavitands in excited state processes has gained momentum recently. Octa acid (OA) has recently been established as an effective reaction vessel in controlling the excited-state chemistry and physics of included guest molecules.<sup>1–5</sup> OA presents several features that separate it from other well-known hosts such as cyclodextrins, cucurbiturils (CB), and calixarenes.<sup>6</sup> In the presence of a guest, OA generally forms a capsular assembly that completely incarcerates the guest molecule and provides better confinement and protection from the aqueous exterior.<sup>7</sup> It absorbs in the region 250–300 nm and has an electron-rich molecular framework and thus upon excitation has a potential to act as an energy and electron donor to the included guest molecules. Most importantly, OA with four tertiary benzylic hydrogens (labeled H<sub>g</sub> in Figure 1) in the internal framework of its cavity can be a hydrogen atom donor to an excited molecule or a reactive intermediate. This investigation focuses on these abstractable hydrogens present at the interior of OA. Although products of reaction between excited guest molecules and cyclodextrin hosts are known,<sup>8,9</sup> no such products have been isolated to date with OA as host. Neither excited carbonyl compounds nor radical intermediates derived from them react with OA. Similarly, highly reactive carbenes generated from adamantanediazirenes that reacted with cyclodextrins only undergo

intramolecular rearrangement within OA.<sup>10a</sup> Cucurbiturils with their secondary and tertiary hydrogens (projecting outside the cavity) are known to be inert toward excited guest molecules and reactive intermediates derived from them.<sup>10b,11–13</sup> This study explores the reactivity of transient intermediate nitrene with the host frameworks of OA and cucurbit[7]uril (CB7).

Photolysis of azidoadamantanes is established to generate reactive nitrenes that undergo intramolecular and intermolecular (solvent) insertion reactions.<sup>14–16</sup> We envisioned that an examination of such systems included within OA and CB7 would provide an opportunity to probe the hydrogen atom donating ability of these hosts. This approach would also afford a route to host cavity functionalization. With these in mind we examined the excited state chemistry of 1-azidoadamantane and 2-azidoadamantane (Figure 1) included within OA and CB7. The nitrenes generated from these azidoadamantanes reacted with OA and produced a covalently linked host–guest product while within CB7 nitrenes yielded products that were noncovalently bound to the host stronger than the reactants. Isolation of the product from CB7 required its displacement

**Special Issue:** Howard Zimmerman Memorial Issue

**Received:** July 16, 2012

**Published:** August 29, 2012

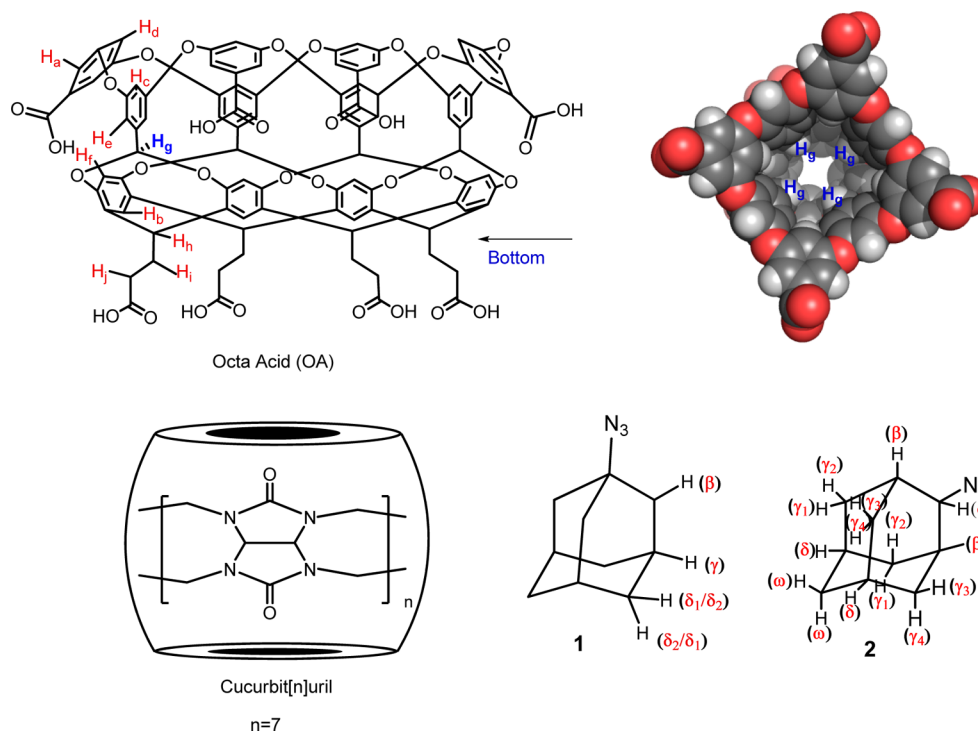


**Figure 1.** Structures of host OA, CB7, and azidoadamantanes used in this study.

with a better binding guest molecule. We present the results with OA first, followed by those with CB7.

## ■ RESULT AND DISCUSSION

**Complexation of Azidoadamantanes with OA.** Both 1-azidoadamantane and 2-azidoadamantane that are sparingly soluble in water formed a highly soluble 1:1 host–guest complex with OA in aqueous borate buffer solution. Complexation was evident from the characteristic upfield shift of the adamantyl hydrogens of these guest molecules (1 and 2) upon inclusion within OA (Figure 2).<sup>17</sup> The host–guest ratio was determined by <sup>1</sup>H NMR titration experiments. As seen in Figures S1 and S2 (Supporting Information, SI), addition of more than 1 equiv of the guest to the host resulted in signals due to uncomplexed guest molecules. The possibility of 1:1 stoichiometry being either a 1:1 cavitandplex or a 2:2 capsuleplex, could be narrowed down by their significantly different diffusion constants in general of  $\sim 1.5 \times 10^{-6} \text{ cm}^2/\text{s}$  and  $\sim 1.2 \times 10^{-6} \text{ cm}^2/\text{s}$ , respectively.<sup>17</sup> Free OA has a diffusion constant closer to  $1.8 \times 10^{-6} \text{ cm}^2/\text{s}$ . With the help of 2D-DOSY experiments the diffusion constants for OA complexes of 1-azidoadamantane and 2-azidoadamantane were determined to be  $1.51 \times 10^{-6} \text{ cm}^2/\text{s}$  and  $1.56 \times 10^{-6} \text{ cm}^2/\text{s}$ , respectively, numbers consistent with a 1:1 cavitandplex in solution.

The complexation behavior was further probed by isothermal titration calorimetric (ITC) measurements.<sup>18</sup> Thermodynamic parameters for complexation of 1 and 2 with OA were determined by monitoring the heat changes during titration of the guest into a host solution (for representative ITC data see Figures S3 and S4 in SI). Since 1 and 2 were not sufficiently soluble in aqueous solution, all ITC experiments were carried out in 50% DMSO + 50% water mixture. The association constant (*K*),  $\Delta G$ ,  $\Delta H$ ,  $\Delta S$ , and stoichiometry of the complex were obtained by fitting the experimental titration curve with the computed one based on an independent binding model

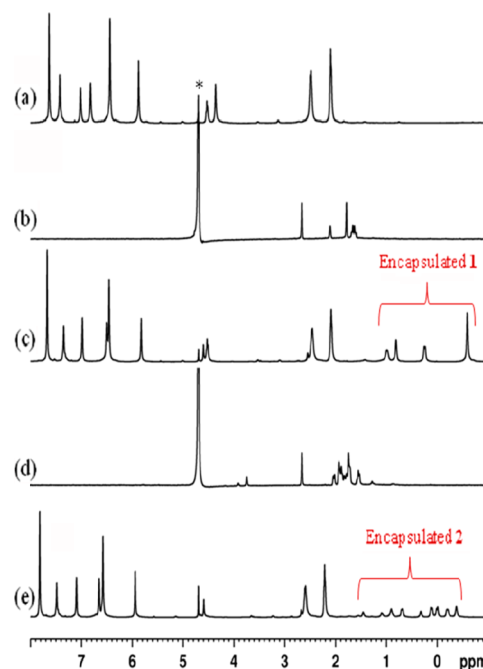


**Figure 2.** <sup>1</sup>H NMR spectra of (a) OA (1 mM, 10 mM sodium tetraborate buffer), (b) 1 mM of 1 in 10 mM sodium tetraborate buffer, (c) 1 in OA (H:G = 1:1, 10 mM sodium tetraborate buffer), (d) 1 mM of 2 in 10 mM sodium tetraborate buffer, and (e) 2 in OA (H:G = 1:1, 10 mM sodium tetraborate buffer).

(Table 1). The binding constants in the range of  $10^5$ – $10^6 \text{ M}^{-1}$  suggested all complexes to be stable in the above solvent mixture. Since the guest inclusion within host OA is driven by a hydrophobic effect, the complexes should be more stable in 100% water in which the photochemical studies were conducted. We believe that the observed high enthalpies of binding ( $\sim$ ca. 8 kcal/mol) result from van der Waals

**Table 1. Binding Constants (K) and Relevant Thermodynamic Parameters for Complexation of 1- and 2-Azidoadamantanes with OA and CB7 at 25 °C**

guest	media	$K_a^a$ ( $M^{-1}$ )	$\Delta G^b$ (kcal/mol)	$\Delta H^c$ (kcal/mol)	$\Delta S^d$ (kcal/mol)	stoichiometry
1	1@OA	$1.95(\pm 0.5) \times 10^6$	$-8.6 \pm 0.1$	$-8.2 \pm 0.3$	$0.4 \pm 0.2$	$0.98 \pm 0.07$
1	1@CB7	$1.2(\pm 0.2) \times 10^6$	$-8.3 \pm 0.1$	$-17.3 \pm 0.3$	$-9.0 \pm 0.5$	$0.90 \pm 0.04$
2	2@OA	$7.04(\pm 0.2) \times 10^5$	$-8.0 \pm 0.02$	$-7.68 \pm 0.1$	$0.3 \pm 0.1$	$0.99 \pm 0.03$
2	2@CB7	$1.4(\pm 0.2) \times 10^6$	$-8.4 \pm 0.1$	$-14.0 \pm 0.2$	$-5.6 \pm 0.3$	$0.90 \pm 0.004$

<sup>a</sup>Mean values measured from at least three ITC experiments at 25 °C in DMSO–water (1:1). Standard deviations are given in parentheses. <sup>b</sup>Gibbs free energy values calculated from  $K_a$  values. <sup>c</sup>Enthalpy values measured by ITC. <sup>d</sup>Entropic contributions to  $\Delta G$  calculated from  $K_a$  and  $\Delta H$  values. A solvent mixture of DMSO and sodium borate buffer in water (1:1) was used for all the titrations.

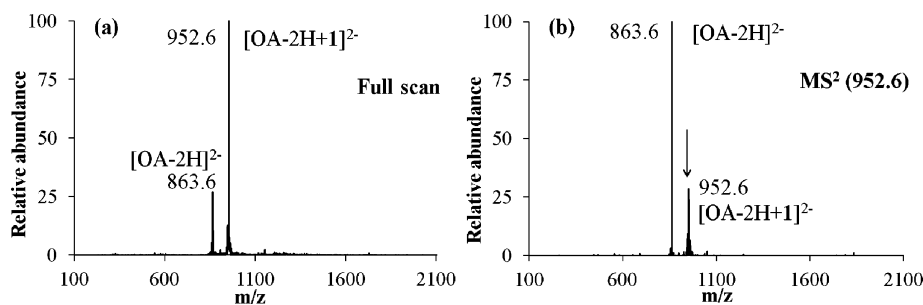


**Figure 3.** ESI-MS of an aqueous solution of 1@OA complexes in the presence of  $NH_3$  ( $1 \mu L/mL$ ): (a) full scan spectrum; (b) fragmentation ( $MS^2$ ) of  $m/z$  952.6 (1@OA). The arrow indicates the fragmented peak. Assignments:  $m/z$  863.6  $[OA - 2H]^{2-}$ ; 952.6  $[OA - 2H + 1]^{2-}$ .

interactions between host and guest. Stoichiometry of the host to guest complex (1:1) inferred from ITC data (Table 1) is consistent with the above  $^1H$  NMR titration and 2D-DOSY results.

Further confirmation for formation of 1:1 complex came from electrospray ionization mass spectrometry (ESI-MS) data. The ESI-MS technique provides valuable information regarding the stoichiometry, reactivity, and binding constants of host–guest complexes as well as of higher order supramolecular assemblies in gas phase.<sup>19–21</sup> Employing ESI-MS studies, we recently reported one of the few examples of gas-phase-stable capsuleplexes (2:2 and 2:1) with octa amine as host.<sup>22</sup> However, to our knowledge, there are no known examples of stable gas phase complexes of OA. Free OA was readily seen in the gas phase under ESI-MS in both negative and positive polarities. The spray of an aqueous solution of OA containing  $NH_3$  ( $1 \mu L/mL$ ) gave rise to peaks at  $m/z$  863.6 ( $[OA - 2H]^{2-}$ ) and 1747.4 ( $[OA + NH_3 + H]^+$ ) in the negative and positive modes, respectively (Figure S5, SI). The addition of 1 to OA gave rise to a new doubly charged ion peaking at  $m/z$  952.6 (Figure 3a) under negative ESI-MS. Its fragmentation led to release of the guest and observation of free OA (Figure 3b). We therefore assign the peak at  $m/z$  952.6 to 1@OA complex. A similar behavior was observed for 2@OA (Figure S6, SI). The azidoadamantane–OA complexes were observed under gentle ionization conditions, namely low desolvation gas flows ( $<2$  L/min) and low capillary exit potentials ( $<150$  V). Under harder ionization conditions (desolvation gas flows  $>2$  L/min and capillary exit potentials  $>150$  V) only free OA was observed, indicating that guest is being released. To our knowledge, this is the first example of a stable gas-phase 1:1 complex of OA host with any guest. As there are no solvent molecules in the gas phase pure hydrophobic effect is absent. The observation of gas-phase stable 1:1 cavitandplexes suggests van der Waals interaction to be likely responsible for the binding and is in agreement with the observed high enthalpies of binding. From the above  $^1H$  NMR, ITC, and ESI-MS studies

it is clear that 1-azidoadamantane and 2-azidoadamantane form stable 1:1 cavitandplexes with OA.

For insight into the orientation of the guest molecules within OA, 2D-COSY, and 2D-NOESY experiments with 1@OA and 2@OA complexes in  $D_2O$  borate buffer solutions were performed. Integration of the peaks and COSY correlations helped us assign the signals due to various guest protons and are indicated in the spectra provided in Figures S7 and S8 (SI). NOESY spectra provided in Figures S9 and S10 (SI) were most helpful to infer the orientation of azidoadamantanes within OA. In both cases, we believe that the  $N_3$  group is pointed toward the tapered bottom part of OA, an arrangement that would place most of the adamantyl protons closer to the opposite, broader rim. This visualization is consistent with the NOESY correlations. For example, in the case of 1-azidoadamantane protons  $\delta_1$  and  $\delta_2$  correlate with  $H_d$  of the host that is present at the broader rim of OA. Consistent with this, proton  $\beta$  that is closer to the  $N_3$  group of the guest correlates with  $H_g$  and  $H_e$  of the host that are present at the bottom and middle of the cavity. Similar analysis in the case of 2-azidoadamantane led us to conclude that the  $N_3$  group is buried at the narrower end of OA. For example, the proton closer ( $\alpha$  and  $\beta$ ) to the  $N_3$  group correlates with  $H_g$  and  $H_e$  of the host. The two protons ( $\gamma$ ) farther away from the  $N_3$  group strongly correlate with  $H_d$  and most importantly show no interaction with  $H_g$ , suggesting that the  $N_3$  group is at the bottom and adamantyl part is at the larger periphery of OA.

To visualize the structure of the two host–guest complexes we generated the most likely structures using the molecular docking program AutoDock Vina.<sup>23</sup> Iterated local search global optimizer with Broyden–Fletcher–Goldfarb–Shanno (BFGS) method was used for the local optimization.<sup>24</sup> A rectangular region,  $10 \text{ \AA} \times 9 \text{ \AA} \times 9 \text{ \AA}$  with a grid spacing of  $1 \text{ \AA}$ , was selected to define the binding site of OA. The atomic partial charges were calculated by the Kollman method, and other docking parameters were set as default. The program determined the total interaction energies between random

pairs of ligands and various selected portions of OA to determine docking poses. For each guest molecule a total of 10 different poses were obtained, and the structures with lowest energy for 1@OA and 2@OA are provided in Figure 4. It is readily seen from these cartoon representations that the N<sub>3</sub> group in these structures is pointed toward the narrower part of OA.

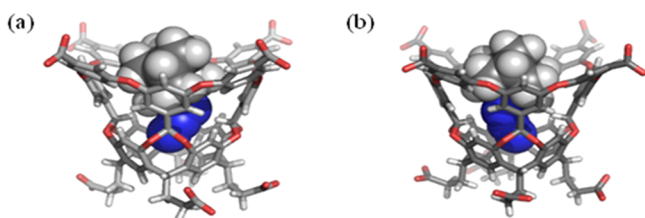


**Figure 4.** Orientations of the azidoadamantanes in (a) 1@OA and (b) 2@OA based on molecular docking study. Color code for atoms: C, gray; N, blue; O, red; H, white.

**Photochemistry of 1-Azidoadamantane@OA and 2-Azidoadamantane@OA Complexes.** Solution photochemistry of 1-azidoadamantane and 2-azidoadamantane is known from literature reports, with 1-azidoadamantane upon photolysis yielding a highly strained reactive imine **4** (characterized only in argon matrix at 12 K) via the nitrene intermediate **3** (Scheme 1a).<sup>14–16,25</sup> In solution, **4** adds to a water molecule to produce aminoalcohol **6** and/or dimerizes to **7**. When complexes of **1** with  $\alpha$ - or  $\beta$ -cyclodextrins were irradiated **6** was obtained as the main product (>90%).<sup>25</sup> Unlike cyclodextrins and cucurbiturils, OA absorbs between 250 and 300 nm (Figure S11, SI). This host therefore has the potential to act as energy and electron donor upon absorption of light and promote the phototransformation of guest molecules that show very low extinction coefficients in this spectral region, such as compounds **1** and **2**. In this study, we are not certain whether 1-azidoadamantane and 2-azidoadamantane included within OA are excited by direct light absorption or via energy transfer following light absorption by OA.

The cavitandplex 1@OA upon irradiation for 40 min ( $\lambda > 280$  nm) showed complete conversion as evident from <sup>1</sup>H NMR spectrum (Figure S12, SI). The <sup>1</sup>H NMR spectrum of the isolated major photoproduct (**5**) contained signals due to OA as well as the adamantyl protons suggestive of the likely reaction of the nitrene generated from 1-azidoadamantane with the host OA (Figure 5). Had a simple noncovalent host–guest complex been formed between an intramolecular nitrene product (**4**) and OA, it would retain the original symmetry, the signals due to OA protons of the isolated product suggested the host to be no longer symmetrical and the likely insertion of the 1-adamantanylnitrene to the molecular frame of OA. 2D-NOESY correlations of the photoproduct (Figure S13, SI) confirmed the interaction between the adamantyl and aromatic groups (signals in the region  $\delta$  0.2 to  $-1.2$  ppm and  $\delta$  5.5 to 8 ppm respectively). Detailed analysis for the presence of  $-\text{NH}$  revealed signals at  $\sim -1.2$  ppm and at  $\sim -0.85$  ppm for the photolyzed 1@OA and 2@OA, respectively. Integration of the signals and COSY interaction analyses indicated the presence of a single  $-\text{NH}$  hydrogen in the photoproduct (see Figure S14, SI). This observation also supports the conclusion that in the major photoproduct the adamantyl group is within the OA cavity and

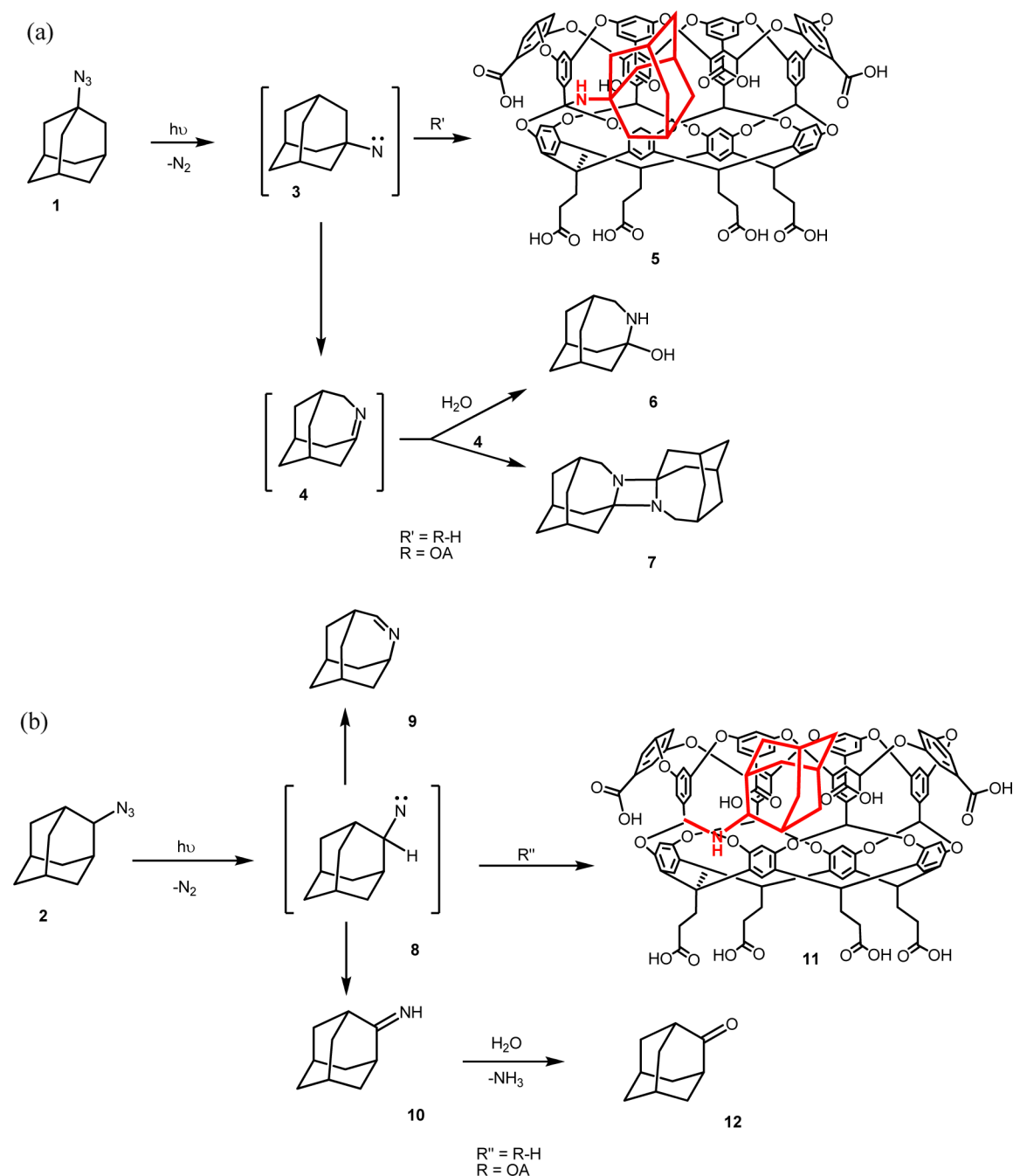
is covalently linked to it. To further confirm that we really have OA-functionalized product, a competitive control experiment with 1-adamantylamine that is likely to form a stronger complex was performed. No displacement of photoproduct occurred. Signals due to 1-adamantylamine in water were observed in the <sup>1</sup>H NMR spectrum. In addition to the OA-functionalized product, a small amount of **6** was also isolated (Table 2).

The photoproduct **5** was further probed by ESI-MS under positive and negative ionization conditions to obtain further support for the conclusion that it is the result of reaction between 1-adamantyl nitrene and OA. Figure 6a presents the mass spectrum of the photoproduct **5** monitored under conditions similar to those used for the detection of 1@OA complex (Figure 3a). A new  $m/z$  value was observed at 938.2 as opposed to 952.6 obtained for 1@OA complex. However, under hard ionization conditions (desolvation gas flows  $>2$  L/min and capillary exit potentials  $>150$  V), unlike 1@OA complex (Figure 3a), the ion at  $m/z$  938.2 was stable, suggesting the formation of a covalently linked system. The fragmentation of  $m/z$  938.2 ( $\text{MS}^2$ ) gave rise to neutral losses of 18 and 44, corresponding to H<sub>2</sub>O and CO<sub>2</sub>, respectively (Figure S15a, SI) a pattern different from that of 1@OA complex, in which the release of the guest and free OA formation was observed (Figure 3b). The fragmentation ( $\text{MS}^2$ ) of the doubly charged negative ion of free OA (Figure S15b, SI) showed the same neutral losses. These observations are consistent with the photoproduct being a result of a chemical reaction between 1-adamantanylnitrene and OA. ESI-MS under positive polarity gave further insight into the structure of the photoproduct. The spray of an aqueous solution of the photoproduct in the presence of NH<sub>3</sub> (1  $\mu\text{L}/\text{mL}$ ) in the positive mode gave rise to a base peak at  $m/z$  1879.6 and to the already observed signal for free OA ( $m/z$  1747.4) (Figure 6b). The isotope distributions obtained using time of flight (TOF) analyzer and the correspondent theoretical patterns near  $m/z$  1879 (Figure S16, SI) are consistent with a product of reaction between the host OA and 1-adamantanylnitrene or a strong noncovalent complex between 1-adamantanylnitrene-derived product and OA. With highly reactive molecules having precedence<sup>26</sup> in being trapped in capsules we fancied that the above mass peak might correspond to a strong noncovalent host–guest complex of the highly reactive **4** with OA. The fragmentations ( $\text{MS}^2$ ) of these two ions (1879 and 1747) are shown in Figure S17 (SI). Unlike the negative ions (Figure S15, SI), the fragmentation of the single positively charged OA and photoproduct are different and reflect the presence of the adamantyl moiety in the photoproduct. While the fragmentation of OA indicates the loss of NH<sub>3</sub> and H<sub>2</sub>O, the major losses in the case of the photoproduct are 135 and 150 Da, corresponding to the adamantyl and amino adamantyl moieties, respectively (see Figure S17, SI).

Based on the above analysis of mass spectral data, we believe that the 1-adamantanylnitrene generated from 1-azidoadamantane has inserted itself at the C–H<sub>g</sub> site of OA, and the most likely structure of the product is the one shown in Scheme 1 a. Formation of this product is consistent with the structure of 1@OA derived from <sup>1</sup>H NMR and molecular modeling. In this structure, the nitrene generated from irradiation of **1** by extrusion of nitrogen would be very close to the four C–H<sub>g</sub> bonds present at the narrower end of the OA cavity. Nitrenes and carbenes attacking the aryl units of cavitands and hemicarcerands and nitrenes inserting into C–H bond of hemicarcerands are known in the literature.<sup>27–29</sup>



Scheme 1. Photolysis Products of (a) 1 and (b) 2



2-Azidoadamantane yields an unstrained imine (major) and adamantanonone (minor) via a nitrene intermediate (Scheme 1 b) in solution and when irradiated as a solid or as inclusion complexes of  $\alpha$ - or  $\beta$ -cyclodextrins in water.<sup>25</sup> However, irradiation of 2-azidoadamantane@OA in aqueous borate buffer solution ( $\lambda > 280$  nm) resulted in a nitrene insertion product **11** similar to **5** with the  $^1H$  NMR spectrum also bearing close similarity to it (Figure 5). Further, NOESY correlations shown in Figure S18 in the SI suggest that the adamantyl and OA parts are linked and the former is tucked inside the later. To probe this further, the ESI-MS of the photoproduct was recorded under positive and negative modes. Under the positive mode, the  $m/z$  value (1878.46), the fragmentation behavior, and the experimental and simulated isotope distributions (Figures S16

and S19, SI) support the conclusion that the photoproduct is **11**. Formation of this product is consistent with the structure of the 2@OA shown in Figure 4. Unstrained imine **9** and adamantanonone **12** were formed as minor products ( $\sim 20\%$ ) (Table 2).

**Complexation of Azidoadamantanes with CB and Their Photochemistry.** Both 1-azidoadamantane and 2-azidoadamantane formed a 1:1 complex with CB7 in water. This conclusion is supported by  $^1H$  NMR titration experiments (Figures S20 and S21, SI) as well as ITC measurements (Table 1 and Figures S22 and S23, SI). The  $^1H$  NMR signals of the guests **1** and **2** included within CB7, as is often the case with most guests, were upfield shifted (Figure 7). Mass spectra recorded by ESI-MS technique gave the mass ion correspond-

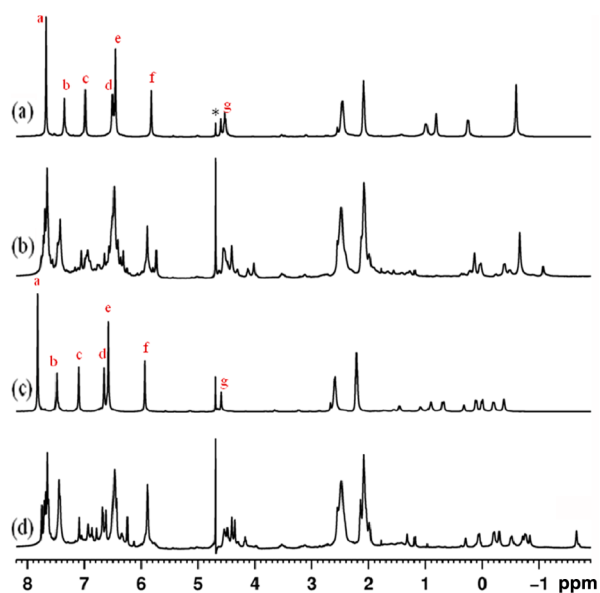


**Figure 5.**  $^1\text{H}$  NMR spectra of (a) **1** in OA (H:G = 1:1,  $[\text{H}] = [\text{G}] = 1$  mM in 10 mM sodium tetraborate buffer), (b)  $^1\text{H}$  NMR spectra of product **1@OA** in  $\text{D}_2\text{O}$  after photolysis followed by extraction with  $\text{CDCl}_3$ ,  $^1\text{H}$  NMR spectra of (c) **2** in OA (H:G = 1:1,  $[\text{H}] = [\text{G}] = 1$  mM in 10 mM sodium tetraborate buffer), (d)  $^1\text{H}$  NMR spectra of product **2@OA** in  $\text{D}_2\text{O}$  after photolysis followed by extraction with  $\text{CDCl}_3$ . \* indicates signal for residual water. For signal assignments of OA, see Figure 1.

**Table 2. Relative Percentages of Products upon Photolysis of Azidoadamantanes in OA and CB7**

guest <sup>a</sup>	media <sup>b</sup>	yield (%)		
		5 <sup>c</sup>	6 <sup>c</sup>	7 <sup>c</sup>
<b>1</b>	alkane solution			88
	<b>1@OA</b>	86	14	
	<b>1@CB7</b>		>95	
		yield (%)		
		9 <sup>c</sup>	11 <sup>c</sup>	12 <sup>c</sup>
<b>2</b>	alkane solution	87		5
	<b>2@OA</b>	19	71	10
	<b>2@CB7</b>	>95		

<sup>a</sup>The samples were irradiated using a medium-pressure mercury lamp (Pyrex tube,  $\lambda > 280$  nm). <sup>b</sup>Products yield were determined by GC after total conversion with adamantane as internal standard. <sup>c</sup>Concentrations of **1** and **2**: OA, CB7 = 1 mM/1 mM.

ing to 1:1 complex (Figures S24, SI). According to ITC measurements, the binding constants were high ( $\sim 10^6 \text{ M}^{-1}$ ),

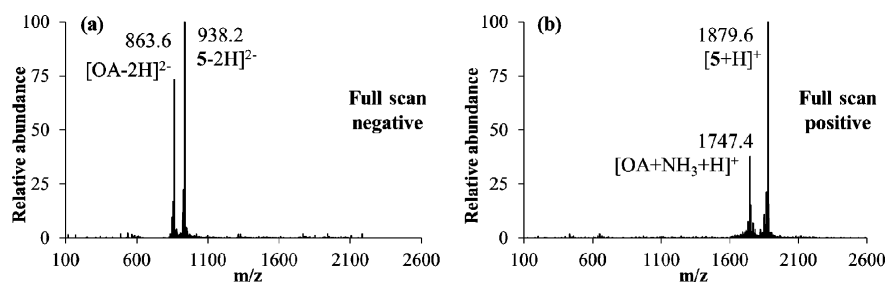


**Figure 6.** ESI-MS spectra (full scans) of (a) photolyzed **1@OA** in the negative polarity, (b) photolyzed **1@OA** in the positive polarity. Assignments:  $m/z$  863.6  $[\text{OA} - 2\text{H}]^{2-}$ ; 938.2  $[\text{5} - 2\text{H}]^{2-}$ ; 1747.4  $[\text{OA} + \text{NH}_3 + \text{H}]^+$ ; 1879.6  $[\text{5} + \text{H}]^+$ .

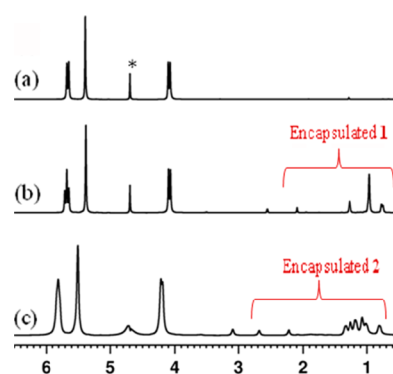


**Figure 7.**  $^1\text{H}$  NMR spectra of (a) CB7 (1 mM, in  $\text{D}_2\text{O}$ ), (b) **1** in CB7 (H:G = 1:1), (c) **2** in CB7 (H:G = 1:1), \* indicates signal for residual water.

and  $\Delta H$  and  $\Delta S$  were more negative than in the case of OA complexes. These suggested that the guests were more tightly held within CB7 and less mobile than within OA. Given the smaller size of CB7 with respect to OA this is not surprising.

Irradiation of **1@CB7** in aqueous solution ( $\lambda > 280$  nm), as per the  $^1\text{H}$  NMR spectrum (Figure 8), gave a new product in

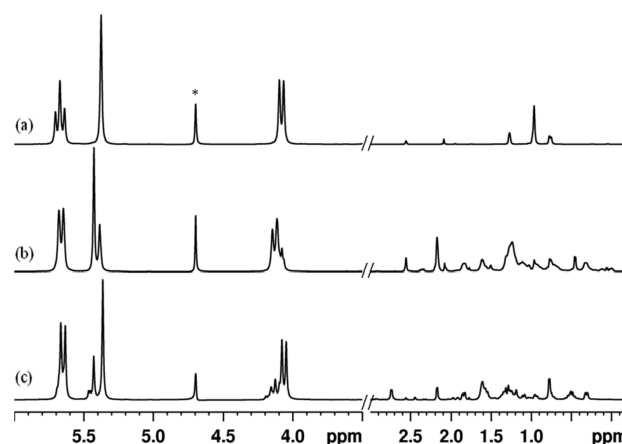


**Figure 8.**  $^1\text{H}$  NMR spectra (500 MHz in  $\text{D}_2\text{O}$ ) of (a) **1** in CB7 (H:G = 1:1,  $[\text{H}] = [\text{G}] = 2$  mM), (b) photoproduct of **1@CB7** after 1 h irradiation, and (c) photoproduct of **1@CB7** after irradiation followed by extraction with  $\text{CDCl}_3$  ( $\lambda > 280$  nm). \* indicates signals due to residual water.

quantitative yield within 1 h. Further characterizations of the product from irradiation similar to those described above to determine complexation of CB7 were carried out (GC and GC-MS, ESI-MS, and  $^1\text{H}$  NMR). GC and GC-MS indicated

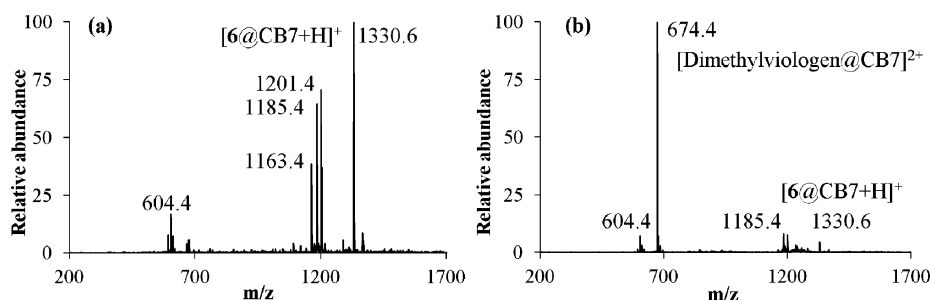


**Figure 9.** ESI-MS spectra (full scans) of (a) photoproduct of 1@CB7 and (b) photoproduct of 1@CB7 in the presence of dimethylviologen<sup>2+</sup>. Assignments:  $m/z$  604.4 [CB7 + 2Na]<sup>2+</sup>; 674.4 [Dimethylviologen@CB7]<sup>2+</sup>; 1163.4 [CB7 + H]<sup>+</sup>; 1185.4 [CB7 + Na]<sup>+</sup>; 1201.4 [CB7 + K]<sup>+</sup>; 1330.6 [CB7 + 6 + H]<sup>+</sup>.

the formation of amino alcohol **6** in small amounts (~10%). The <sup>1</sup>H NMR spectrum of the aqueous extract consisted of signals due to both CB7 and the adamantyl part of the guest (Figure 8). The ESI-MS spectrum of the extract of 1@CB7 showed a major peak at  $m/z$  1330.6 (Figure 9a), a value corresponding to a system containing both **6** and CB7. To get further insight into the nature of this ion we performed MS/MS studies. The fragmentation of  $m/z$  1330.6 gave rise to a major peak at 1312.6, which corresponds to the loss of H<sub>2</sub>O, together with free CB7 at  $m/z$  1163.4 and further fragmentation of former leading to the breaking of the remaining guest and release of CB7 (Figure S25, SI). The release of guest fragments upon fragmentation of CB host–guest complexes has been reported when the binding is strong.<sup>30,31</sup> These results could mean either CB7 was functionalized with 1-adamantyl nitrene or **6** was tightly held within CB7. Interestingly when the ESI-MS of the extract was recorded after the addition of dimethyl viologen<sup>2+</sup> the signal at 1330.6 gave rise to a new signal at 674.4 corresponding to dimethyl viologen<sup>2+</sup>@CB7 complex (Figure 9b), a result we interpreted as displacement of the photoproduct that was tightly held within CB7. The <sup>1</sup>H NMR spectrum recorded to probe if this displacement could occur in solution showed noticeable but partial displacement. Addition of 1-adamantylamine, known to bind to CB7 with much higher binding constant than dimethyl viologen<sup>2+</sup>,<sup>32,33</sup> to the irradiated mixture resulted in total displacement of the product **6** to produce 1-adamantylamine@CB7 exclusively as detected by <sup>1</sup>H NMR (Figure 10) and **6** could be quantitatively extracted with CDCl<sub>3</sub> (Figure 10). Thus, irradiation of 1@CB7 in water ( $\lambda > 280$  nm) gave quantitatively the amino alcohol **6** that was held tightly and could only be extracted by displacement. Unlike in the case of OA there was no reaction of 1-azidoadamantyl nitrene and CB7.

Similar to 1@CB7, irradiation of 2@CB7 in aqueous solution gave a new set of <sup>1</sup>H NMR signals that remained even after extraction with CDCl<sub>3</sub> (Figure S26, SI). Based on ESI-MS data of the irradiated sample in the absence and presence of dimethyl viologen<sup>2+</sup> and on the fragmentation of the ion at  $m/z$  1312.6 (Figure S27, SI), we concluded that the photoproduct **9** is tightly held within CB7. Thus, irradiation of 2@CB7 gave **9** quantitatively, and there was no reaction between 2-adamantyl nitrene and CB7. The photobehaviors of both **1** and **2** are identical within CB7, and no functionalization of the host could be carried out with highly reactive nitrenes. This result is not unexpected if the hydrogens' location on the exterior of CB7 is considered. The experience with **1** and **2** within CB7 has demonstrated that one needs to be careful in isolating products of photoreactions. It is quite likely that in

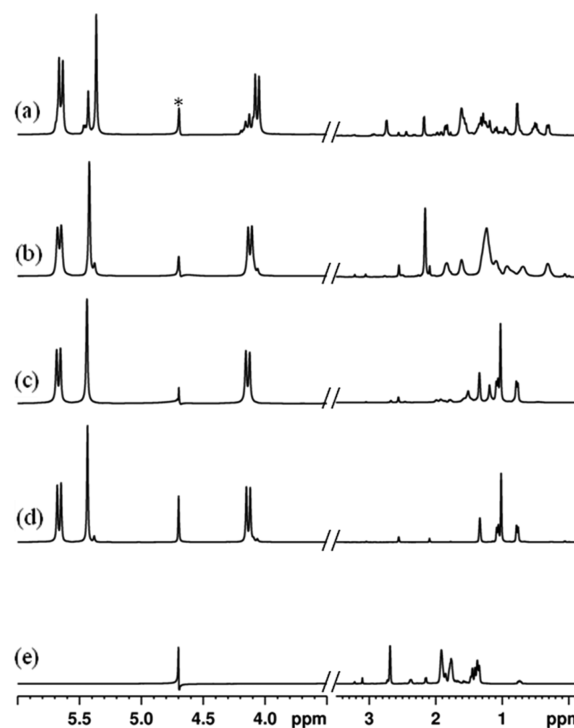


**Figure 10.** <sup>1</sup>H NMR spectra (500 MHz in D<sub>2</sub>O) of (a) 1@CB7 after photolysis followed by extraction with CDCl<sub>3</sub>, (b) **6** in CB7 (H:G = 1:1, [H] = [G] = 2 mM), (c) addition of 1 equiv of 1-adamantylamine in (a), (d) 1-adamantylamine in CB7 (H:G = 1:1, [H] = [G] = 2 mM), and (e) **6** in D<sub>2</sub>O. \* indicates signals due to residual water.

some cases the product might bind so strongly to the host and that exchange with a more powerful guest would be the only way to separation.

## SUMMARY

Supramolecular control of photoreactions requires a thorough understanding of the reaction cavity in which a reaction is being carried out. This study is focused toward understanding the reactivity of two hosts, namely OA and CB7. Thus far, both are known to be inert toward an excited molecule and a reactive intermediate derived from it. The interior of octa acid contains four hydrogens that could be susceptible for abstraction by an excited carbonyl compound, a radical, or a carbene. Thus far, none of them are reported to react with the host OA. We have shown in this presentation that nitrenes generated by photolysis of azidoadamantanes undergo intermolecular C–H insertion and thereby get attached to OA. As far as we are

aware this is the first report demonstrating that OA is not as inert as it is believed to be. This observation suggests that one needs to be watchful when using OA as the host. Along with OA, we have been employing cucurbiturils as reaction cavities in our research. In this case, the abstractable hydrogens are at the exterior. As expected, there was no functionalization of CB when photolysis of azidoadamantanes included in CB was carried out. However, we were surprised to note that the product was noncovalently bound to the host and could not be extracted by conventional means. The product had to be displaced with the help of a stronger binding guest. The two observations we have reported here highlight the challenges in applying the concepts of supramolecular chemistry in carrying out selective photoreactions in molecular containers.

## ■ EXPERIMENTAL SECTION

**Materials.** Hosts octa acid, cucurbit[7]uril and azidoadamantanes, and 3-hydroxy-4-azatricyclo[4.3.1.1]undecane (**6**) were prepared as reported in literature.<sup>6,34,35</sup> All other chemicals of the highest available purity were purchased from commercial suppliers.

**Nature of the Complexes Probed by 1D <sup>1</sup>H NMR and 2D DOSY NMR experiments.** To 0.6 mL of a D<sub>2</sub>O solution of host OA (1 mM OA in 10 mM Na<sub>2</sub>B<sub>4</sub>O<sub>7</sub>) in an NMR tube were added increments of 0.25 equiv of guests (2.5 μL of a 60 mM solution in DMSO-*d*<sub>6</sub>) followed by a 5 min sonication after each addition, and <sup>1</sup>H NMR recorded. Formation of the complex was monitored by the gradual increase in intensity of bound guest signals. After addition of 1.25 equiv of guest, signals due to free, unbound guest were observed. To a solution of 0.6 mL of 1 mM of CB7 in D<sub>2</sub>O was added 10 μL of a 60 mM guest solution, the solution was shaken vigorously for 5 min, and the NMR spectra were recorded.

The diffusion constants (D) of the complexes were determined by diffusion ordered spectroscopy (DOSY), a technique useful in separation based on <sup>1</sup>H NMR signals and, in particular, as a supramolecular entity is expected to diffuse slower than the smaller individual components. All diffusion experiments were performed on a 500 MHz NMR instrument at 25 °C. The concentration of both host and guest was 1 mM in 10 mM sodium tetraborate buffer. Formation of the complexes was monitored by adding guests (2.5 μL of a 60 mM solution in DMSO-*d*<sub>6</sub>) to a host solution (1 mM in 10 mM sodium tetraborate buffer) followed by sonication for 5 min.

**Experimental Procedure for Photolysis and Characterization of Products.** Photolysis was performed by irradiation with a medium-pressure mercury lamp (450 W) of guest@host complex in sodium tetraborate buffer solution contained in a Pyrex tube (λ > 280 nm), after purging with nitrogen for 30 min. The conversion was confirmed by comparison of the <sup>1</sup>H NMR spectrum of the solution prior to irradiation and 1D <sup>1</sup>H NMR spectroscopy post irradiation. Complete conversion of reactants to products was observed for 1@OA and 2@OA complexes after irradiation for 40 min (λ > 280 nm), while 1–2@CB7 solutions were irradiated for 1 h. After the irradiation, the products were extracted five times using CDCl<sub>3</sub> and dried over anhydrous sodium sulfate. The CDCl<sub>3</sub> solution was concentrated to approximately 0.1 mL and was injected into the GC. The GC program used for OA samples: starting at 70 °C, held (for 1 min for OA and 2 min for CB7), applying ramp of 10 °C per min, up to 270 °C, held for 10 min. All reactions were repeated (at least three times) for consistency. The product solution was injected into a GC–MS. The molecular weight obtained from the molecular ion peak and the fragmentation pattern confirmed the identity of the products. Comparison with authentic sample further confirmed the identity of the products. On the other hand, the aqueous extract was concentrated to 0.6 mL and further 1D and 2D NMR (COSY, NOESY) experiments were performed.

**Isothermal Titration Calorimetric Study.** The equilibrium constants and thermodynamic parameters for the inclusion of azidoadamantanes in both OA and CB[7] were determined using an isothermal titration calorimeter. All titrations were performed at 25 °C

while stirring at 350 rpm. Electrical calibrations were performed before each experiment. Nanoanalyze software was used to calculate the equilibrium constant and standard molar enthalpy of reaction from the titration curve. Each microcalorimetric titration experiment consisted of 40–60 successive injections. In each titration, a constant volume (6 μL/injection) of guest solution was injected into the reaction cell (969 μL) charged with host solution. A standard solution of the host and guest in deionized water–DMSO mixture was diluted to provide a working solution at 0.1 to 0.15 mM and 1 to 2 mM respectively. The titrations were performed in 50% DMSO–water solution. The heat of dilution was calculated as the difference between the data from the last 10 injections (heat generated due to the dilution of the guest into solvent mixture (DMSO + water)) and those of the host–guest titration. The accuracy of the calculated thermodynamic quantities for the 1:1 complexation was checked by performing several independent titration runs. The reported standard deviation was obtained from the Nanoanalyze software.

**Guest Orientation through Molecular Docking.** Molecular docking (predicting the preferred orientation of one molecule to a second when bound to each other to form a stable complex) of the guest molecules with the OA was performed using AutoDock Vina. An algorithm called Iterated Local Search global optimizer with the Broyden–Fletcher–Goldfarb–Shanno (BFGS) method was used for the local optimization according to the interatomic potentials of all atom types present in the host and guest molecules, including the 12–6 Lennard-Jones potentials for van der Waals interactions and coulomb potentials for electrostatic interactions. The program determined the total interaction energies between random pairs of ligands and various selected portions of host capsule to determine docking poses. A grid map of dimension 10 Å × 9 Å × 9 Å with a grid spacing of 1 Å was placed to cover the OA capsular assembly. The atomic partial charges were calculated by the Kollman method and other docking parameters were set as default. For each guest molecule a total of 10 different poses were obtained and of the various structures generated, the ones with the lowest energy in each case are reported.

**Mass Spectrometry. Sample Preparation.** The ESI-MS studies of OA and OA photoproducts were performed using 100 μM aqueous solutions prepared with Milli-Q water containing 1 μL/mL of ammonia. The host–guest complexes were prepared in a 1:1 ratio at 100 μM concentration and using a 50 mM stock solution of each guest in DMSO and Milli-Q water with 1 μL/mL of ammonia. The solutions were sonicated for 10 min and allowed to equilibrate for 30 min before analysis. The complexes were also prepared by addition of a single crystal of the solid guest to a 100 μM solution of the host, followed by sonication for 30 min and equilibration overnight. Similar spectral distributions were obtained for both methods but the signal intensities are lower when DMSO is used. The CB7 complexes were prepared by addition of a single crystal of the solid guest to a 100 μM solution of the host, followed by sonication for 30 min and equilibration overnight.

**ESI-MS System.** ESI-MS spectra were obtained using mass spectrometers equipped with time-of-flight (TOF) and ion trap analyzers. The ions were continuously generated by infusing the aqueous sample solution into the source at 4 μL/min. The solutions were studied in the negative and positive polarities. For the observation of host–guest complexes of OA soft desolvation conditions are required. Typical experimental conditions for the observation of these host–guest complexes in negative polarity were: capillary voltage (CE): 3.0 kV; capillary exit voltage: –80 V; skimmer voltage: –15 V; drying gas temperature: 300 °C; drying gas flow: 1 L/min; nebulizer gas pressure: 40 psi. Host–guest complexes with CB7 can be observed under positive polarity in the following conditions: capillary voltage (CE): –4.0 kV; capillary exit voltage: 105 V; skimmer voltage: 35 V; drying gas temperature: 300 °C; drying gas flow: 6 L/min; nebulizer gas pressure: 30 psi. The photoproducts with OA as well as the host–guest complexes of the photoproducts with CB7 can be seen in a with range of spray and ion optics conditions. Typically the main parameters in the positive polarity were: capillary voltage (CE): –4.0 kV; capillary exit voltage: 300 V; skimmer voltage: 100 V; drying gas: 300 °C at 6 L/min; nebulizer gas pressure: 40 psi.



**Preparation of Compounds 5 and 11. Compound 5.**

Compound 5 was obtained after photolysis of 1@OA complexes by irradiation with a medium-pressure mercury lamp (450 W) in sodium tetraborate buffer contained in a Pyrex tube ( $\lambda > 280$  nm), after purging with nitrogen for 30 min. After irradiation, the products were extracted five times using  $\text{CDCl}_3$ . The organic layer was discarded and the aqueous extract was concentrated to 0.6 mL and further 1D and 2D NMR (COSY, NOESY) experiments were performed.  $^1\text{H}$  NMR (500 MHz,  $\text{D}_2\text{O}$ )  $\delta_{\text{H}}$ : -0.94 (1H), -0.65 (6H), -0.4 (3H), 0.05 (3H), 0.18 (3H), 2.1 (8H), 2.5 (8H), 4.4 (2H), 5.7–5.9 (6H), 7.6–7.8 (9H). HRMS (ESI): calcd for the first peak of the isotope series of  $\text{C}_{106}\text{H}_{80}\text{O}_{32}\text{N} [\text{M} + \text{H}]^+$  1878.4658, found 1878.4543.

**Compound 11.** Compound 11 was prepared following the procedure described for compound 5 but using 2@OA complexes.  $^1\text{H}$  NMR (500 MHz,  $\text{D}_2\text{O}$ )  $\delta_{\text{H}}$ : -1.7 (2H), -0.9 (1H), -0.85 (2H), -0.75 (1H), -0.55 (2H), -0.35 (2H), -0.2 (2H), 0.4 (1H), 1.35 (1H), 2.1 (8H), 2.5 (8H), 5.9 (4H). HRMS (ESI): calcd for the first peak of the isotope series of  $\text{C}_{106}\text{H}_{80}\text{O}_{32}\text{N} [\text{M} + \text{H}]^+$  1878.4658, found 1878.4454.

**■ ASSOCIATED CONTENT****■ Supporting Information**

$^1\text{H}$  NMR titration spectra, ITC data, ESI-MS of host–guest complexes and photoproducts, 2-D COSY and NOESY spectra of host–guest complexes, and Cartesian coordinates for docked host–guest structures. This information is available free of charge via the Internet at <http://pubs.acs.org>.

**■ AUTHOR INFORMATION****Corresponding Author**

\* (J.P.D.S.) Tel: 351 289 800900. E-mail: [jpsilva@ualg.pt](mailto:jpsilva@ualg.pt) (V.R.) Tel: 305 2841534. E-mail: [murthy1@miami.edu](mailto:murthy1@miami.edu).

**Notes**

The authors declare no competing financial interest.

**■ ACKNOWLEDGMENTS**

V.R. is grateful to the National Science Foundation for generous financial support (CHE-0848017) and for funds toward the purchase of an LC-ESI-MS (CHE-0946858). J.P.S. thanks the Portuguese Foundation for Science and Technology (Grant No. REEQ/717/QUI/2005). V.R. thanks U. Brinker (University of Vienna) for useful discussions.

**■ REFERENCES**

- (1) Ramamurthy, V.; Parthasarathy, A. *Isr. J. Chem.* **2011**, *51*, 817.
- (2) Parthasarathy, A.; Ramamurthy, V. *Photochem. Photobiol. Sci.* **2011**, *10*, 1455.
- (3) Sundaresan, A. K.; Ramamurthy, V. *Photochem. Photobiol. Sci.* **2008**, *7*, 1555.
- (4) Gibb, C. L. D.; Sundaresan, A. K.; Ramamurthy, V.; Gibb, B. C. J. *Am. Chem. Soc.* **2008**, *130*, 4069.
- (5) Natarajan, A.; Kaanumalle, L. S.; Jockusch, S.; Gibb, C. L. D.; Gibb, B. C.; Turro, N. J.; Ramamurthy, V. *J. Am. Chem. Soc.* **2007**, *129*, 4132.
- (6) Gibb, C. L. D.; Gibb, B. C. J. *Am. Chem. Soc.* **2004**, *126*, 11408.
- (7) Porel, M.; Jayaraj, N.; Kaanumalle, L. S.; Maddipatla, M. V. S. N.; Parthasarathy, A.; Ramamurthy, V. *Langmuir* **2009**, *25*, 3473.
- (8) Brinker, U. H.; Buchkremer, R.; Kolodziejczyk, M.; Kupfer, R.; Rosenberg, M.; Poliks, M. D.; Orlando, M.; Gross, M. L. *Angew. Chem., Int. Ed.* **1993**, *32*, 1344.
- (9) Krois, D.; Brecker, L.; Werner, A.; Brinker, U. H. *Adv. Synth. Catal.* **2004**, *346*, 1367.
- (10) (a) Gupta, S.; Choudhury, R.; Krois, D.; Wagner, G.; Brinker, U. H.; Ramamurthy, V. *Org. Lett.* **2011**, *13*, 6074. (b) Gupta, S.; Choudhury, R.; Krois, D.; Brinker, U. H.; Ramamurthy, V. *J. Org. Chem.* **2012**, *77*, 5155.

(11) Masson, E.; Ling, X.; Joseph, R.; Kyeremeh-Mensah, L.; Lu, X. *RSC Adv.* **2012**, *2*, 1213.

(12) Lagona, J.; Mukhopadhyay, P.; Chakrabarti, S.; Isaacs, L. *Angew. Chem., Int. Ed.* **2005**, *44*, 4844.

(13) Lee, J. W.; Samal, S.; Selvapalam, N.; Kim, H.-J.; Kim, K. *Acc. Chem. Res.* **2003**, *36*, 621.

(14) Quast, H.; Eckert, P. *Liebigs Ann. Chem.* **1974**, *1974*, 1727.

(15) Dunkin, I. R.; Shields, C. J.; Quast, H.; Seiferling, B. *Tetrahedron Lett.* **1983**, *24*, 3887.

(16) Radziszewski, J. G.; Downing, J. W.; Jawdosiuik, M.; Kovacic, P.; Michl, J. *J. Am. Chem. Soc.* **1985**, *107*, 594.

(17) Jayaraj, N.; Zhao, Y.; Parthasarathy, A.; Porel, M.; Liu, R. S. H.; Ramamurthy, V. *Langmuir* **2009**, *25*, 10575.

(18) Rekharsky, M. V.; Inoue, Y. *Chem. Rev.* **1998**, *98*, 1875.

(19) Zadnani, R.; Kraft, A.; Schrader, T.; Linne, U. *Chem.—Eur. J.* **2004**, *10*, 4233.

(20) Kogej, K.; Schalley, C. A. *Analytical Methods in Supramolecular Chemistry*; John Wiley & Sons: Chichester, 2007.

(21) Rozhenko, A. B.; Schoeller, W. W.; Letzel, M. C.; Decker, B.; Avena, C.; Mattay, J. *Chem.—Eur. J.* **2006**, *12*, 8995.

(22) Da Silva, J. P.; Kulasekharan, R.; Cordeiro, C.; Jockusch, S.; Turro, N. J.; Ramamurthy, V. *Org. Lett.* **2012**, *14*, 560.

(23) Trott, O.; Olson, A. J. *J. Comput. Chem.* **2010**, *31*, 455.

(24) Nocedal, J.; Wright, S. J. *Numerical Optimization*, 2nd ed.; Springer Verlag: Berlin, 1999.

(25) Brinker, U. H.; Walla, P.; Krois, D.; Arion, V. B. *Eur. J. Org. Chem.* **2011**, *2011*, 1249.

(26) Warmuth, R. *Eur. J. Org. Chem.* **2001**, *2001*, 423.

(27) Lu, Z.; Moss, R. A.; Sauer, R. R.; Warmuth, R. *Org. Lett.* **2009**, *11*, 3866.

(28) Wagner, G.; Arion, V. B.; Brecker, L.; Krantz, C.; Mieusset, J.-L.; Brinker, U. H. *Org. Lett.* **2009**, *11*, 3056.

(29) Warmuth, R.; Makowiec, S. *J. Am. Chem. Soc.* **2007**, *129*, 1233.

(30) Da Silva, J. P.; Jayaraj, N.; Jockusch, S.; Turro, N. J.; Ramamurthy, V. *Org. Lett.* **2011**, *13*, 2410.

(31) Jayaraj, N.; Porel, M.; Ottaviani, M. F.; Maddipatla, M. V. S. N.; Modelli, A.; Da Silva, J. P.; Bhogala, B. R.; Captain, B.; Jockusch, S.; Turro, N. J.; Ramamurthy, V. *Langmuir* **2009**, *25*, 13820.

(32) Liu, S.; Ruspic, C.; Mukhopadhyay, P.; Chakrabarti, S.; Zavalij, P. Y.; Isaacs, L. *J. Am. Chem. Soc.* **2005**, *127*, 15959.

(33) Kim, H. J.; Jeon, W. S.; Ki, Y. H.; Kim, K. *Proc. Natl. Acad. Sci. U.S.A.* **2002**, *99*, 5007.

(34) Day, A.; Arnold, A. P.; Blanch, R. J.; Snushall, B. *J. Org. Chem.* **2001**, *66*, 8094.

(35) Sasaki, T.; Eguchi, S.; Katada, T.; Hiroaki, O. *J. Org. Chem.* **1977**, *42*, 3741.